New insight into knockout reactions from the two-proton halo nucleus ^{17}Ne

F. Wamers,[1] C. Lehr,[2] J. Marganiec-Gałązka,[2,3] F. Aksouh,[1,4] Yu. Aksyutina,[1] H. Álvarez-Pol,[5] L. Atar,[2] T. Aumann,[1,2]
S. Beceiro-Novo,[5] C. A. Bertulani,[6] K. Boretzky,[1] M. J. G. Borge,[7] C. Caesar,[1,2] M. Chartier,[8] A. Chatillon,[1] L. V. Chulkov,[1,9]
D. Cortina-Gil,[10] P. Díaz Fernández,[11] H. Emling,[1] O. Ershova,[1,12] L. M. Fraile,[13] H. O. U. Fynbo,[14] D. Galaviz,[7] H. Geissel,[1]
M. Heil,[1] M. Holl,[11] H. T. Johansson,[11] B. Jonson [11] C. Karagiannis,[1] O. A. Kiselev,[1] J. V. Kratz,[15] R. Kulessa,[16] N. Kurz,[1]
C. Langer,[1,12,17] M. Lantz,[18] T. Le Bleis,[1] R. Lemmon,[19] Yu. A. Litvinov,[1] K. Mahata,[1] C. Müntz,[1] T. Nilsson,[11] C. Nociforo,[1]
V. Panin,[1,2] S. Paschalis,[8,20] A. Perea,[7] R. Plag,[1,12] R. Reifarth,[1,12] A. Richter,[2] K. Riisager,[14] C. Rodriguez-Tajes,[10] D. Rossi,[1,2]
D. Savran,[1] H. Scheit,[1] G. Schrieder,[2] H. Simon,[1] J. Stroth,[12] K. Sümmerer,[1] O. Tengblad,[7] S. Typel,[1,2] and H. Weick[1]

[1]*GSI Helmholtzzentrum für Schwerionenforschung GmbH, D-64291 Darmstadt, Germany*
[2]*Institut für Kernphysik, Technische Universität, D-64289 Darmstadt, Germany*
[3]*National Centre for Nuclear Research, Radioisotope Centre POLATOM (POLATOM), Andrzeja Sołtana 7, 05-400 Otwock, Poland*
[4]*Physics and Astronomy Department, College of Sciences, King Saud University, 2689 Riyadh, 12372 Saudi Arabia*
[5]*Departamento de Física de Partículas, Universidade de Santiago de Compostela, ES-15782 Santiago de Compostela, Spain*
[6]*Department of Physics and Astronomy, Texas A&M University-Commerce, Texas 75429, USA*
[7]*Instituto de Estructura de la Materia, CSIC, ES-28006 Madrid, Spain*
[8]*Department of Physics, University of Liverpool, Liverpool L69 3BX, United Kingdom*
[9]*NRC Kurchatov Institute, RU-123182 Moscow, Russia*
[10]*Universidade de Santiago de Compostela, 15782 Santiago de Compostela, Spain*
[11]*Fysiska institutionen, Chalmers Tekniska Högskola, SE-41296 Göteborg, Sweden*
[12]*Institut für Angewandte Physik, Goethe Universität, D-60438 Frankfurt am Main, Germany*
[13]*Department of Atomic, Molecular and Nuclear Physics, Universidad Complutense de Madrid, ES-28040 Madrid, Spain*
[14]*Department of Physics and Astronomy, University of Aarhus, DK-8000 Aarhus, Denmark*
[15]*Institut für Kernchemie, Johannes Gutenberg-Universität Mainz, D-55122 Mainz, Germany*
[16]*Instytut Fisiki, Uniwersytet Jagelloński, PL-30–059 Kraków, Poland*
[17]*University of Applied Sciences Aachen, D-52066 Aachen, Germany*
[18]*Institutionen för fysik och astronomi, Uppsala Universitet, SE-75120 Uppsala, Sweden*
[19]*Nuclear Physics Group, STFC Daresbury Laboratory, Warrington WA4 4AD, Cheshire, United Kingdom*
[20]*Department of Physics, University of York, York YO10 5DD, United Kingdom*

Background: The unexplained disagreement in the dependence of spectroscopic factors (C^2S_{exp}) on the binding energy obtained by nucleon knockout using different targets is still a puzzle that needs to be addressed.

Purpose: To find an explanation of this riddle through exclusive measurements using different targets.

Method: The exclusive measurements were performed by using a ^{17}Ne beam with an energy of 500 MeV/u incident on C and CH_2 targets. Through the standard theoretical approach, C^2S_{exp} were derived from the analysis of the experimental data on proton ejection from the proton halo in ^{17}Ne as well as from its core ^{15}O.

Result: For the C target, proton ejection from the proton halo gave C^2S_{exp} about 37% smaller than for the H target. But when protons are ejected from the core of ^{17}Ne, C^2S_{exp} are identical within statistical uncertainties.

Conclusion: An explanation for the difference in C^2S_{exp} could be the removal of both halo protons, a more important reaction pathway for the C target. The C^2S_{exp} values obtained by analyzing the proton ejection from the core indicate that it is not affected by the interaction with the halo protons.

I. INTRODUCTION

The present paper is motivated by the need to improve the interpretation of nucleon knockout reaction cross sec-

tions obtained experimentally. The longstanding, puzzling discrepancy between spectroscopic factors, obtained in experiments with light reaction targets (^{9}Be, ^{12}C) and those obtained with hydrogen targets [1], remains an open question. In the experiments with light reaction targets a strong dependence between the experimental cross section, and hence the resulting spectroscopic factors, C^2S_{exp}, and the difference between the proton and neutron binding energies, $\Delta S = S_p - S_n$ is found. This dependence essentially disappears in experiments employing H targets.

When target nuclei heavier than hydrogen are used, two different reaction mechanisms for nucleon knockout are usually considered [2]: (i) Stripping, which is the dominant one, and (ii) diffraction dissociation. In stripping, the nucleon is removed from the projectile by quasifree nucleon-nucleon scattering [3], while diffraction dissociation is a process in which the incoming reaction partner receives a small transverse pulse and is fragmented, while the target remains intact. In the case of a hydrogen target, the contribution to the reaction from diffraction dissociation is negligible [4]. In our recent paper [5], the cross sections of single proton removal from ^{17}Ne in the C and H targets were compared, choosing, in the case of the C target, only the stripping of one proton from the two-proton halo of ^{17}Ne. The spectroscopic factor of proton knockout from the ^{17}Ne proton halo on the H target was obtained as 2.08(10). This is, within statistical uncertainty equal to 2, as expected for a nucleus with a two proton halo. However, for the C target, this value is only 1.502(35), indicating that diverse reaction mechanisms lead to a decrease in the single-proton detachment cross section. Secondary collisions of an incoming or knocked-out nucleon inside the core also lead to a decrease in the nucleon knockout cross section and, consequently, to a decrease in $C^2 S_{exp}$ [6–8], but without strong correlation with ΔS, which must be present to solve the puzzle.

It was shown experimentally [5] that the mechanism of knocking out a valence proton from a ^{17}Ne beam impinging a carbon target leads to simultaneous knocking out of nucleons from the target with a probability of 69.8(2.3)%. Thus, the reason for the observed reduction of $C^2 S$ within carbon-induced knockout may lie in the importance of secondary interactions of nucleons knocked out from the target. This can be investigated by studying the knockout of protons from the ^{15}O core of ^{17}Ne.

II. EXPERIMENTAL SETUP

The present experiment was performed at the R^{3}B/LAND setup at the GSI Radioactive Beam Facility. The details of how the experiment setup was designed have been described in our earlier papers [9,10]. A schematic representation of the detectors used is shown in Fig. 1. The ^{17}Ne beam, with an energy of 500 MeV/u, was selected with the FRS fragment separator and directed towards a reaction target, consisting of either polyethylene (CH$_2$) with thickness 213(5) mg/cm^2 or carbon (C) with thickness 370(7) mg/cm^2. This gave the possibility to extract data corresponding to pure hydrogen (H) by subtracting data collected with the pure C target from the CH$_2$ target data.

The γ spectra were measured in coincidence with ^{15}O and a proton moving at forward angles with multiplicity $p_{mult} = 1$ (see Fig. 1). The possibility of choosing $p_{mult} = 1$ is ensured by the high proton detection efficiency of the time-of-flight wall, 99.3(5). Corrections have been made for ^{15}O + 2p events misidentified as ^{15}O + 2p. In the cases when several γ rays passed through the Crystal Ball simultaneously, the γ ray with the highest deposited energy was chosen. This leads to a significant reduction in background from random γ-ray coincidences.
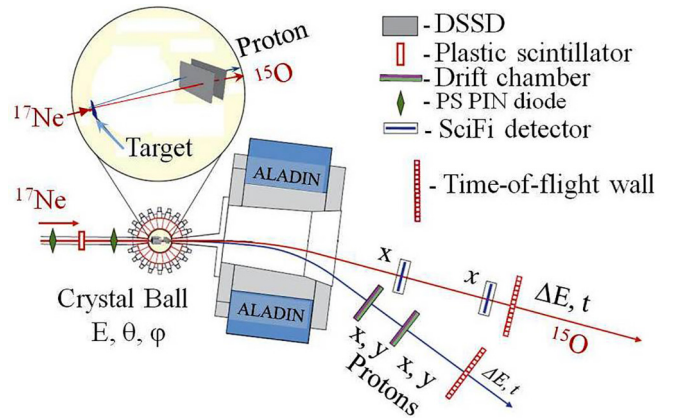

FIG. 1. Schematic view of the R^{3}B/LAND setup at GSI. The quantities measured with the various detectors of the setup are indicated. DSSD stands for double-sided silicon strip detector, SciFi for scintillation fiber detector and PS PIN for position sensitive pin diodes. For more details, see text.

Two sources of background were considered: the interaction of the beam with materials surrounding target, which was determined with an empty target, and reactions that are accompanied by γ rays stemming from excited states in the ^{15}O fragments. The measured γ-radiation spectra were corrected for Doppler shifts.

The experimental response function and geometric acceptance were obtained from R^{3}BRoot, the simulation and analysis framework for R3B experiments [11]. These simulations include the setup geometry, detector resolution, and beam parameters. All experimental data were corrected for geometrical acceptance and detection efficiency.

The given uncertainties are statistical. Systematic errors, due to uncertainties in target thickness and detection efficiencies of the protons and charged fragments, are of the order of 3%. When γ-ray detection in the Crystal Ball is required, the systematic uncertainty of the experimental cross sections is about 6%.

III. NEGATIVE AND POSITIVE PARITY STATES IN THE ^{15}O-PROTON RELATIVE ENERGY SPECTRUM

### A. Energy levels of ^{16}F

The energy level diagram for ^{16}F is shown in Fig. 2.

In the 0–3 MeV energy region, the four negative parity states have the single-particle structure: proton plus ^{15}O(g.s.). The proton orbital $1s_{1/2}$ splits into 0^- and 1^- multiplet, and the $0d_{5/2}$ orbital splits into 2^- and 3^- multiplet due to the interaction of proton with odd neutron $0p_{1/2}$ in ^{15}O [12].

These states can be populated by proton knockout from the proton halo of ^{17}Ne. In the energy region 3–7 MeV, four states with positive parity are known. The 3^+ state indicates a single-particle structure with ^{15}O $\otimes \pi(1f_{7/2})$ as its main component [13,14]. This state cannot be populated by the capture of valence protons after proton knockout from the ^{15}O core of ^{17}Ne.

For the three states $I^\pi = 1_1^+$, 2^+, and 1_2^+ states, respectively, the single-particle configuration ^{15}O $\otimes \pi(1p)$ is very
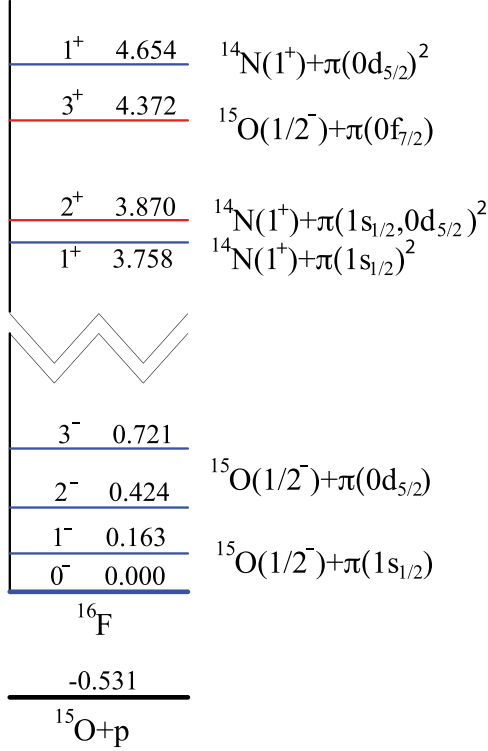
FIG. 2. Energy level diagram for ^{16}F.

small, less than 5% [15,16]. The structure of the $I^\pi = 2^+$ consists of mixed ^{14}N$(1^+) \otimes \pi(1s\,0d)$ configuration. The absorption of two protons from the proton halo of ^{17}Ne is unlikely for this state.

The two states 1_1^+ and 1_2^+ are highly excited in the two-proton transfer reaction ^{14}N$(1^+)(^3$He$, n)$, reflecting the structures ^{14}N$(1^+) \otimes \pi(1s_{1/2})^2$ and ^{14}N$(1^+) \otimes \pi(0d_{5/2})^2$ [15,17]. It is these two states that have the highest probability of capturing two protons from the proton halo in ^{17}Ne.

B. Relative energy spectra

Relative energy spectra in ^{15}O $+ p$ after knocking out a proton from ^{17}Ne in C and H targets are shown in Fig. 3. The spectra were obtained in coincidence by detecting ^{15}O and one proton under the requirement of multiplicity $p_{\text{mult}} = 1$. Negative parity states in ^{16}F were populated by knocking a proton out of the proton halo of ^{17}Ne, while excitation of positive parity states by ejection of a proton from ^{15}O, the core of ^{17}Ne. The fit to the spectrum performed separately in two energy regions at 0–3 MeV and at 3–7 MeV. Excitation energies and resonance widths in the low-energy region were taken from [18]. The experimental resolution was also taken into account. The tails from resonances in this energy region were used in fitting two other resonances with $I^\pi = 1^+$ in the high energy region. The widths of these resonances are ruled by experimental resolution. The curves in Fig. 3 show the results of the fitting.

In the energy region $0 < E_{fp} \leqslant 3$ MeV, the fitting parameters are the sums of cross sections $\sigma_{01} = \sigma(0^-) + \sigma(1^-)$,
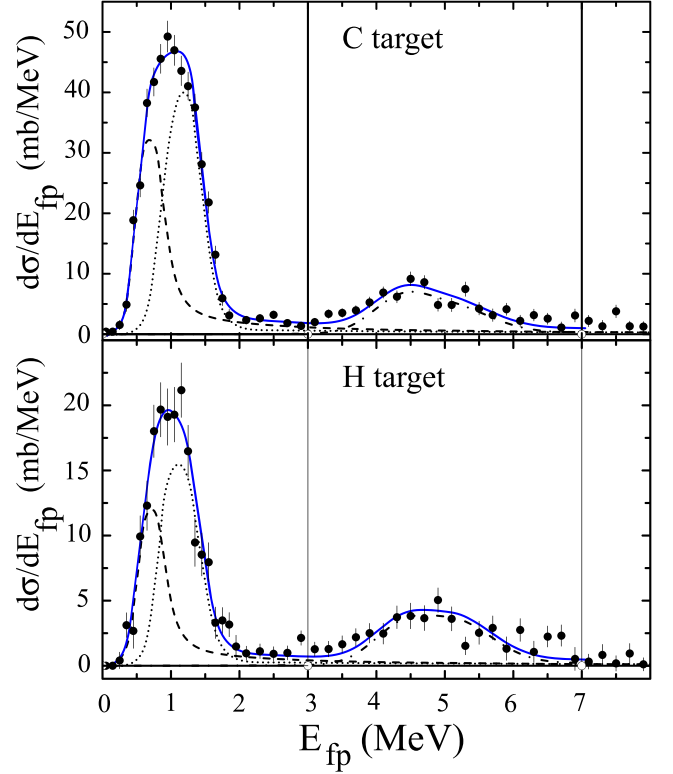

FIG. 3. Relative energy spectra $d\sigma/dE_{fp}$ obtained in coincidence between ^{15}O and a proton ($p_{\text{mult}} = 1$) at forward angles after knocking out a proton from ^{17}Ne in reactions with the C or H targets. The fits shown are described in the text.

(dashed line in Fig. 3), $\sigma_{23} = \sigma(2^-) + \sigma(3^-)$ (dotted line), and their ratios $\sigma(0^-)/\sigma(1^-)$, $\sigma(2^-)/\sigma(3^-)$. For states with positive parity, the fitting parameters are are $\sigma_{12}^+ = \sigma(1_1^+) + \sigma(1_2^+)$ (dashed-doted line) and $\sigma(1_1^+)/\sigma(1_2^+)$. The derived cross sections are summarized in Table I.

In the case of the H target, the ratios of the cross sections σ_0/σ_1 and σ_2/σ_3 are proportional to $2I + 1$ within statistical uncertainty, as expected. For the C target, the obtained ratio of cross sections for the excitation of 0^- and 1^- states is close to the $2I + 1$ ratio, but the ratio of cross sections for the excitation of 2^- and 3^- states deviates significantly from the expected ratio of 5/7.

C. Spectroscopic factors

The key quantity in the interpretation of the experimental cross sections is the calculated single-particle cross section σ_{sp}

TABLE I. Cross sections (mb) for population of resonances in ^{16}F, measured in coincidence with ^{15}O and a proton under forward angles with $p_{\text{mult}} = 1$. See text for details.

	negative parity			positive parity	
σ_{01}	σ_0/σ_1	σ_{23}	σ_2/σ_3	σ_{12}^+	σ_1^+/σ_2^+
C 24.3(1.2)	0.386(90)	30.1(1.2)	0.465(77)	12.49(79)	1.22(20)
H 8.8(1.0)	0.20(14)	12.0(1.0)	0.75(20)	7.74(70)	1.26(36)

TABLE II. Spectroscopic factors $C^2 S_{\exp}$ for $^{15}O \otimes \pi (1s_{1/2})^2$ and $^{15}O \otimes \pi (0d_{5/2})^2$ configurations in ^{17}Ne(g.s.).

Target	$1s_{1/2}$ $C^2 S_{\exp}$	$0d_{5/2}$ $C^2 S_{\exp}$	Sum of $C^2 S_{\exp}$
C	0.527(26)	0.977(39)	1.504(47)
H	0.755(86)	1.31(10)	2.06(13)

corresponding to one proton plus the residue, in its ground or excited state. The σ_{sp} values are then used to convert the measured partial cross-sections into experimental spectroscopic $C^2 S_{\exp}$ factors using

$$C^2 S_{\exp} = \frac{\sigma_{\exp}}{\sigma_{sp}}. \qquad (1)$$

The σ_{sp} calculations were based on the MOMDIS code [19] for the C target and on the code described in Ref. [4] for the H target. The eikonal approximation was used to calculate separately the cross sections for stripping and diffraction dissociation. The diffraction dissociation is negligible for the H target and contributes with 7–8 % of the proton removal cross section for the C target. The spectroscopic factors, given in Table II, agree with those in Ref. [5].

The values of cross sections and spectroscopic factors correspond, within statistical uncertainty, to the values obtained in [5]. The fit was performed with a fixed ratio of cross sections equal to the $2I + 1$ ratio. Thus, the conclusion that the experimentally obtained spectroscopic factor for protons in the proton halo of ^{17}Ne is close to 2 in the H-target measurements and 30% smaller in the C target measurements is confirmed. The cross sections, σ_{01} and σ_{23}, for the C target must be increased with 10.3 mb for both reaction pathways to obtain $C^2 S_{\exp}$ values similar of those for the H target. Thus, the decrease of the cross sections for the C target does not depend on the orbits of the protons in the halo.

The simultaneous removal of the two protons from the halo can be considered as the cause of the decrease in the values of $C^2 S_{\exp}$, but the contribution from this process should not depend appreciably on the orbital of the removed protons.

IV. EXCITED STATES OF ^{15}O POPULATED BY CAPTURE OF VALENCE PROTONS

A. Excited states of ^{15}O with configuration $^{14}N(T = 0) + p$

The level scheme of ^{15}O is shown in Fig. 4. The proton binding energy in ^{15}O is 7.30 MeV, and states at higher energy are proton unstable.

The three states at 6.79 MeV ($I^\pi = 3/2^+$), 6.86 MeV ($I^\pi = 5/2^+$) and 7.28 MeV ($I^\pi = 7/2^+$) have single-particle structures based on ^{14}N(g.s.) core: $^{14}N(1^+) \otimes \pi (1s_{1/2})^2$ and $^{14}N(1^+) \otimes \pi (0d_{5/2})^2$. The states at 6.86 MeV and 7.28 MeV are de-excited via the 5.24 MeV ($I^\pi = 5/2^+$) state [20] as shown in Fig. 4. The state $I^\pi = 3/2^+$ at 6.79 MeV de-excites directly into the ground state ^{15}O.

The measurement of the $^{14}N(p, \gamma)^{15}O$ cross section [21] shows that the proton absorption leading to the ^{15}O states at 6.86 MeV, $I^\pi = 5/2^+$, and 7.28 MeV, $I^\pi = 7/2^+$, is negligible.

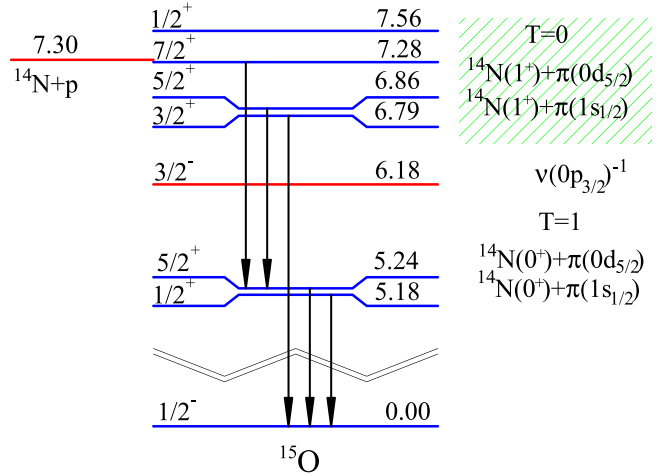FIG. 4. Energy level diagram for ^{15}O.

The $3/2^-$ state at 6.18 MeV is explained to be $p_{3/2}^{-1}$ state produced by raising a $0p_{3/2}$ neutron to the $0p_{1/2}$ shell [22]. This level cannot be populated by proton capture from the halo of ^{17}Ne by $^{14}N(1^+)$.

Thus, the only state that can be strongly populated by the absorption of a single proton remains the $I^\pi = 3/2^+$ state at 6.79 MeV. The proton capture occurs at orbital momenta $\ell = 0$, $C^2 S = 0.51(11)$, and $\ell = 2$, $C^2 S = 0.16(3)$ [23].

B. Excited states of ^{15}O with configuration $^{14}N(T = 1) + p$

The lowest $T = 1/2$ states of ^{15}O at 5.18 MeV ($I^\pi = 1/2^+$) and 5.24 MeV ($I^\pi = 5/2^+$) have predominantly mixed single-particle structure $1/3^{14}N(T = 1) \otimes \pi (1s_{1/2}) + 2/3^{14}O \otimes \nu (1s_{1/2})$ for the $1/2^+$ state and $1/3^{14}N(T = 1) \otimes \pi (0d_{5/2}) + 2/3^{14}O \otimes \nu (0d_{5/2})$ for the $5/2^+$ state (see Ref. [24] and references therein). The halo protons in ^{17}Ne occupy the $1s_{1/2}$ and $0d_{5/2}$ orbitals, so after proton stripping from its core, these two states can be strongly populated by one proton capture from the proton halo.

C. Bremsstrahlung

Measurements of the γ spectra from excited states of ^{15}O, populated after the proton knockout from the ^{15}O core by the capture of valence protons in ^{14}N faces the problem of the incredibly huge background caused by random coincidences of bremsstrahlung radiation with ^{15}O and proton. The constraints imposed on the relative energy between ^{15}O and the proton allows the shape of this background to be revealed. The request $E_{fp} < 1.4$, highlighting the region of the spectrum $d\sigma / dE_{fp}$ with maximum cross section, Fig. 3, where the contribution of random coincidences is close to 100%, yielded a nearly pure spectrum of bremsstrahlung radiation, Fig. 5.

Knowledge of the shape of the bremsstrahlung spectrum will greatly simplify the fit of the gamma-ray spectrum and reduce the statistical uncertainties of the resulting cross sections for excited states.

We first discuss the origin of this background. Many efforts, both experimental and theoretical, have been made to
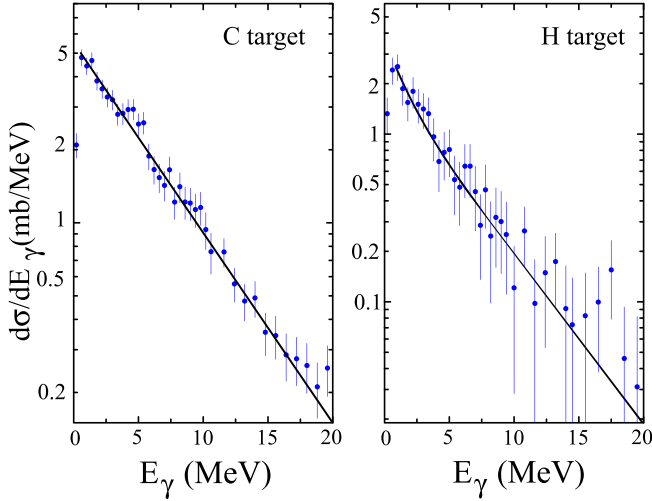
FIG. 5. Differential cross section $d\sigma/dE_\gamma$ for the bremsstrahlung γ radiation in the beam-at-rest system obtained for $E_{fp} < 1.4$ MeV.

FIG. 6. Differential cross section in the beam-at-rest system for the detected γ rays coincident with $^{15}O + p$ in the final state for $E_{fp} \geqslant 1.4$ MeV from the C and H targets.

understand the mechanism of photon production in various reactions with heavy ions at incident energies up to 120 MeV/u (see Ref. [25] for a review). These studies have shown that the main mechanism for the production of high-energy γ rays is related to the sudden deceleration or deflection of charged particles traveling through matter inside the electric fields of atomic nuclei. As a result of these studies, it was found that photons can be either direct or thermal. Direct photons arise at an early stage of the compression reaction. Thermal bremsstrahlung is radiation emitted by ionized gas of a plasma in thermal equilibrium at a certain temperature, and has a softer energy spectrum than the direct photons.

In the present experiment, the energy of the γ spectrum is limited to 20 MeV, and the dominant component of the bremsstrahlung emission is due to thermal photons. The shape of the energy spectra from these photons can be described with an exponential function as

$$\frac{d\sigma}{dE_\gamma} = \frac{\sigma}{E_0} \exp\left(-\frac{E_\gamma}{E_0}\right), \qquad (2)$$

where σ is the cross-section value and E_0 is a slope parameter. The beam energy in this experiment is 500 MeV/u, which is about four times higher than in Ref. [25], but the bremsstrahlung spectrum still has an exponential character, as shown in Fig. 5. The fit gave $E_o = 5.26(13)$ MeV and $E_o = 2.47(25)$ MeV for the C and H targets, respectively. These values of the slope parameter E_o correspond to thermal photons. For comparison, the γ spectrum of thermal photons obtained by colliding a ^{40}Ca beam with an energy of 120 MeV/u with a ^{40}Ca target [25] gave a value of $E_0 = 6.87$ MeV.

D. Population of excited states in ^{15}O after proton ejection from the core of ^{17}Ne

The γ spectra in the beam-at-rest system obtained using the C and H targets are shown in Fig. 6. The red solid lines represent the background caused by random coincidences with
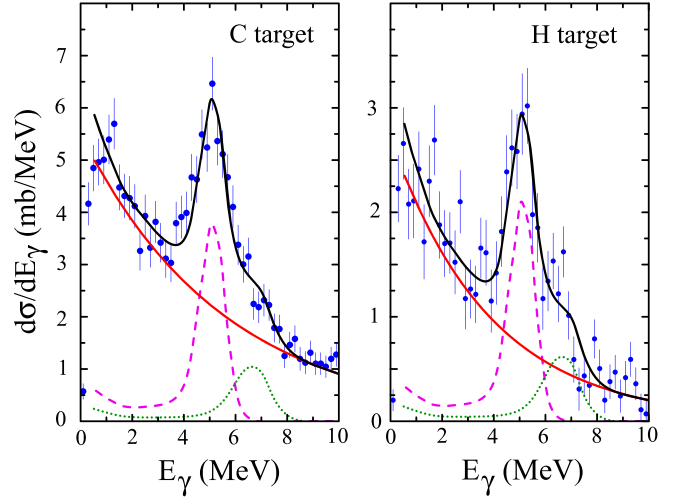
the bremsstrahlung radiation, the dashed curves refer to the two overlapping states in ^{15}O at 5.18 MeV ($I^\pi = 1/2^+$) and 5.24 MeV $I^\pi = 5/2^+$) while the dot curves pertain to the state at 6.79 MeV ($I^\pi = 3/2^+$). The random-coincidence background is described by Eq. (2) with $E_o = 5.26$ MeV for the C target and 2.47 MeV for the H target (see Fig. 5). The quality of the fit gave χ^2/N values of 1.06 for the C target and 1.17 for the H target. The cross sections obtained for the excitation of the resonances are summarised in Table III.

The fraction of true coincidences of γ rays with $^{15}O + p$ events in the relative energy spectrum, $d\sigma/dE_{fp}$, was obtained by selecting coincidences within the energy range $3 \leqslant E_\gamma \leqslant 8$ MeV (see Fig. 6) and subtracting it from the random coincidences.

The result is shown in Fig. 7. These spectra, which have a similar nonresonant shape for both targets, show that the unabsorbed proton flies away without any resonance-like structures and confirm the mechanism of capture of only one proton from the two-proton halo.

V. RESULTS OF THE ANALYSIS OF THE OBTAINED EXPERIMENTAL DATA

The principal points and stages in the evolution of the ^{17}Ne remnants after proton knockout from its ^{15}O core are summarized in Fig. 8. A proton ejecting out of the core of ^{17}Ne forms ^{14}N in either the ground ($I^\pi = 1^+$, $T = 0$) or in the first excited ($I^\pi = 0^+$, $T = 1$) state, surrounded by two

TABLE III. Cross sections (mb) for different types of γ-rays from ^{15}O, obtained in coincidence with ^{15}O and proton ($p_{\mathrm{mult}} = 1$) at small angles.

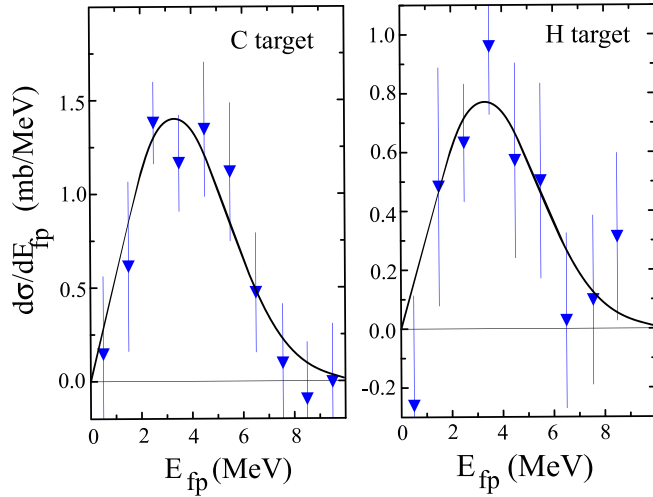| Target	$\sigma(1/2^+) + \sigma(5/2^+)$	$\sigma(3/2^+)$
Carbon	6.33(41)	2.61(33)
Hydrogen	3.53(80)	1.52(24)

FIG. 7. Relative energy spectra of ^{15}O-p in the proton knockout from ^{15}O followed by a proton absorption from the proton halo in ^{17}Ne, leading to the occupation of γ-decaying states in ^{15}O, from the C and H targets. The solid lines provide guides to the eye.

protons from the proton halo. The absorption of a single proton from the proton halo by the ^{14}N(0^+) leads to populating $T = 1/2$ states of ^{15}O at 5.18 MeV ($I^\pi = 1/2^+$) and 5.24 MeV ($I^\pi = 5/2^+$), which have a predominantly single-particle structure of ^{14}N(0^+) $\otimes \pi(1s_{1/2})$ and ^{14}N(0^+) $\otimes \pi(0d_{5/2})$.

The absorption of a single proton from the halo by the ^{14}N(1^+) leads to populating the $T = 1/2$ state at 6.79 MeV ($I^\pi = 3/2^+$). The relative energy spectra of ^{15}O-p accompanying the absorption of a single proton from the proton halo in ^{17}Ne show nonresonant behavior (see Fig. 5).
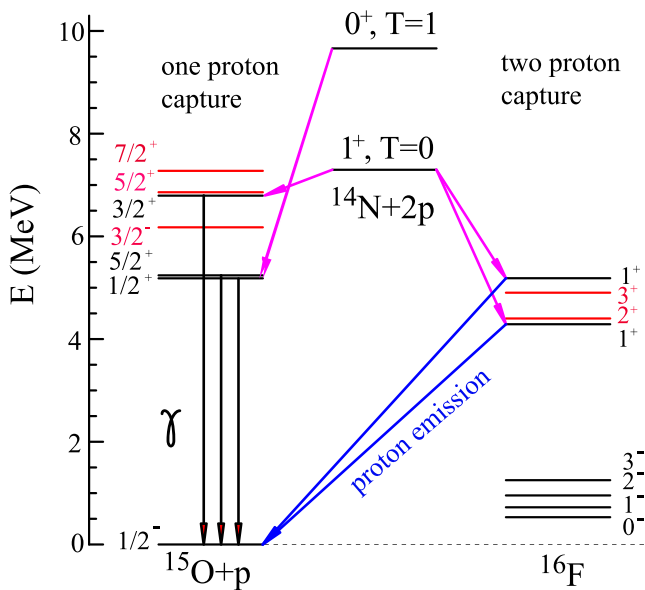

FIG. 8. Reaction branches accompanying a proton knockout from ^{15}O, the core of ^{17}Ne. States weakly populated or unpopulated by proton absorption are shown in red.

TABLE IV. Cross sections (mb) for proton removal from ^{15}O, the core of ^{17}Ne. Experimental spectroscopic factors $C^2 S_{exp}$ are obtained from calculated single-particle knockout cross sections σ_{sp}, Ref. [4] for the H target, and Ref. [19] for the C target. Theoretical spectroscopic factors $C^2 S_{th}$ are taken from [26]. R_s is the ratio $C^2 S_{exp}/C^2 S_{th}$.

^{14}N($I^\pi = 1^+, T = 0$) + p				
Target	σ_{exp}	σ_{sp}	$C^2 S_{exp}$	$C^2 S_{th}$	R_s
Carbon	15.10(59)	25.77	0.586(23)	0.797	0.735(29)
Hydrogen	9.26(74)	16.58	0.559(44)	0.797	0.701(56)
^{14}N($I^\pi = 0^+, T = 1$) + p				
Target	σ_{exp}	σ_{sp}	$C^2 S_{exp}$	$C^2 S_{th}$	R_s
Carbon	6.33(41)	23.76	0.266(17)	0.405	0.657(42)
Hydrogen	3.53(80)	15.81	0.223(51)	0.405	0.55(13)

The absorption of two protons from the proton halo by ^{14}N(1^+) leads to two states with $I^\pi = 1^+$: ^{14}N(1^+) $\otimes \pi(1s_{1/2})^2$ and ^{14}N(1^+) $\otimes \pi(0d_{5/2})^2$. It turns out that this gives additional information about the halo structure of ^{17}Ne. The low energy state ^{16}F(1_1^+) at 3.758 has a ^{14}N(1^+) $\otimes \pi(1s^{1/2})^2$ structure, while the state ^{16}F(1_2^+) at 4.654 MeV has a ^{14}N(1^+) $\otimes \pi(0d^{5/2})^2$ structure. The excitation cross sections of these states reflect the two-proton halo structure in ^{17}Ne. The σ_1^+/σ_2^+ ratios are, within statistical uncertainty, equal for both the C target, 1.22(20), and the H target, 1.26(36) (see Table I). The ratio of proton removal cross section from the two-proton halo of ^{17}Ne, σ_{23}/σ_{01} is equal to 1.239(79) for the C target and 1.36(19) for the H target. Thus, the proton stripping from the ^{17}Ne gives also information on the structure of the proton halo in this nucleus. Note that the results derived using different targets are consistent with each other. This fact helps to explain the difference in the experimental spectroscopic factors obtained for different targets in Ref. [5], where the $C^2 S_{exp}$ for the C target gave the value of 30% lower than that for the H target. A possible reason for this discrepancy is the absence in the calculation of σ_{sp} of the simultaneous ejection of two protons from the proton halo, a process that is obviously more significant when a heavier target is used.

The experimental cross sections for the formation of ^{14}N($I^\pi = 1^+, T = 0$) and ^{14}N($I^\pi = 0^+, T = 1$) with a proton ejected from the core of ^{17}Ne on different targets are given in Table IV.

The theoretical spectroscopic factors $C^2 S_{th}$ given in Table IV are taken from the Ref. [26]. Spectroscopic factors for ^{14}N(1^+) + p and ^{14}N(0^+) + p configurations in ^{15}O were calculated using interactions with three characteristic parts $0p$ shell, cross shell, and $1s0d$ shell [27] in the large-scale shell calculation code KSHELL [28]. Comparison of the spectroscopic factors $C^2 S_{th}$ and $C^2 S_{exp}$ resulted in quenching factors $R_s = C^2 S_{exp}/C^2 S_{th}$ which are within statistical uncertainties the same for different ^{14}N + p configurations and targets, with the mean value 0.66(4). Note also that the obtained spectroscopic factors also remain unchanged within the statistical uncertainties. No dependence on the target was observed.

The cross section of ^{14}N nuclei produced in fragmentation reactions induced by a ^{15}O beam with 308 MeV/u energy directed at the C target have been obtained by Boillos [29].

This cross section was used by Sun [26] to derive the inclusive quenching factor. The calculations which includes 13 different configuration in the ^{15}O structure gave quenching factor $R_s = 0.63(6)$. Measurements at close energy, but with the H target [30], gave $R_s = 0.76(9)$ [31]. Both values are in agreement within experimental uncertainties with the values obtained in the present experiment (see Table IV). The similar values of R_s obtained for proton striking either out of the core of ^{17}Ne or from ^{15}O show that the core is free of appreciable interaction with the proton halo.

However, calculations within the standard Distorted Wave Impulse Approximantion (DWIA) formalism [32] also based on data from Ref. [30] gave $R_s = 1.05(19)$. The obtained R_s values are compared to calculations of another type, which give noticeably smaller values (see Figs. 1 and 2 in Ref. [32]). It is stated in Ref. [32] that the lack of proper consideration of higher order effects becomes more significant in the inclusive type of cross section measurements involving numerous reaction branches. In contrast, the present experiment uses exclusive measurements of proton ejection from the core of ^{17}Ne, leading to only two reaction pathways with ^{14}N in either the ground or the first excited state

VI. CONCLUSION

The experimental single-particle spectroscopic factors C^2S_{exp} obtained when proton is knocked out of ^{15}O, as the core of ^{17}Ne, are within statistical uncertainties independent of the target type.

The obtained quenching factors coincide within experimental uncertainty with the data obtained by proton knockout from free ^{15}O. This confirms that the ^{15}O core inside the two-proton halo nucleus ^{17}Ne is not perturbed by the interaction with protons from the halo.

The study of proton knockout from the core of ^{17}Ne shows a branched reaction process leading, in particular, to excited states with positive parity in the unbound ^{16}F. This indicates that the interpretation of the experimental data based on the knockout of strongly bound nucleon may encounter difficulties in inclusive measurements.

A comparison of experimental data on proton ejection from the proton halo ^{17}Ne obtained using different targets demonstrated good agreement with the shell model when using the H target. However, spectroscopic factors obtained using the C target revealed significant quenching, which is attributed to the associated process, the simultaneous knockout of both protons from the halo. While for nucleon knockout from weakly bound nuclei the reduction of the spectroscopic factor is much stronger when using the H target (see Fig. 56 in Ref. [1]

The discrepancy in spectroscopic factors measured using different targets has become an enigma that is posed as one of the key problems of nuclear physics that needs to be solved. In the review paper [1], it was proposed to give a relevant answer to the question, what new experimental data are needed to solve this problem and to guide theory? As a starting point to address this problem, exclusive measurements of nucleon knockout from weakly bound nuclei with simultaneous use of different targets in the study are needed. The puzzle has come up analyzing inclusive measurements in which numerous reaction pathways lead to the same final result. Exclusive experiments, such as [5,10] and described in the present paper, will reduce the ambiguities in the analysis of the experimental data.

[1] T. Aumann, C. Barbieri, D. Bazin, C. A. Bertulani, A. Bonaccorso, W. H. Dickhoff *et al.*, Prog. Part. Nucl. Phys. **118**, 103847 (2021).

[2] D. Bazin, R. J. Charity, R. T. de Souza, M. A. Famiano, A. Gade, V. Henzl *et al.*, Phys. Rev. Lett. **102**, 232501 (2009).

[3] V. Panin, M. Holl, J. T. Taylor, Y. Aksyutina, H. Alvarez-Pol, T. Aumann *et al.*, Phys. Lett. B **797**, 134802 (2019).

[4] T. Aumann, C. A. Bertulani, and J. Ryckebusch, Phys. Rev. C **88**, 064610 (2013).

[5] F. Wamers, C. Lehr, J. Marganiec-Gałązka, F. Aksouh, Yu. Aksyutina, H. Álvarez-Pol *et al.*, Eur. Phys. J. A **59**, 154 (2023).

[6] C. A. Bertulani, Phys. Lett. B **846**, 138250 (2023).

[7] M. Gómez-Ramos, J. Gómez-Camacho, and A. M. Moro, Phys. Lett. B **847**, 138284 (2023).

[8] T. Pohl, Y. L. Sun, A. Obertelli, J. Lee, M. Gómez-Ramos, K. Ogata *et al.*, Phys. Rev. Lett. **130**, 172501 (2023).

[9] V. Panin, J. T. Taylor, S. Paschalis, F. Wamers, Y. Aksyutina, H. Álvarez-Pol *et al.*, Phys. Lett. B **753**, 204 (2016).

[10] C. Lehr, F. Wamers, F. Aksouh, Yu. Aksyutina, H. Álvarez-Pol, L. Atar *et al.*, Phys. Lett. B **827**, 136957 (2022).

[11] D. Bertini, J. Phys.: Conf. Ser. **331**, 032036 (2011).

[12] C. R. Hoffman, B. P. Kay, and J. P. Schiffer, Phys. Rev. C **94**, 024330 (2016).

[13] H. Fuchs, H. Homeyer, H. Oeschler, R. Lipperheide, and K. Möhring, Nucl. Phys. A **196**, 286 (1972).

[14] A. Fazely, B. D. Anderson, M. Ahmad, A. R. Baldwin, A. M. Kalenda, R. J. McCarthy, J. W. Watson *et al.*, Phys. Rev. C **25**, 1760 (1982).

[15] N. H. Hamann, Nucl. Phys. A **433**, 198 (1985).

[16] W. A. Sterrenburg, S. Brandenburg, J. H. van Dijk, A. G. Drentje, M. B. Greenfield, M. N. Harakeh, H. Riezebos, H. Sakai, W. Segeth, S. Y. van der Werf, and A. van der Woude, Nucl. Phys. A **420**, 257 (1984).

[17] W. Bohne, H. Fuchs, K. Grabisch, D. Hilscher, U. Jahnke, H. Kluge, and T. G. Masterson, Phys. Lett. B **47**, 342 (1973).

[18] I. Stefan, F. de Oliveira Santos, O. Sorlin, T. Davinson, M. Lewitowicz, G. Dumitru *et al.*, Phys. Rev. C **90**, 014307 (2014).

[19] C. Bertulani and A. Gade, Comput. Phys. Commun. **175**, 372 (2006).

[20] Y. S. Horowitz, D. B. McConnell, J. Ssengabi, and N. Keller, Nucl. Phys. A **151**, 161 (1970).

[21] A. Lemut, D. Bemmerer, F. Confortola, R. Bonetti, C. Broggini, P. Corvisiero *et al.*, Phys. Lett. B **634**, 483 (2006).

[22] J. Keinonen, M. Bister, and A. Anttila, Nucl. Phys. A **286**, 505 (1977).

[23] P. F. Bertone, A. E. Champagne, M. Boswell, C. Iliadis, S. R. Hale, V. Y. Haper, and D. C. Powell, Phys. Rev. C **66**, 055804 (2002).

[24] H. T. Fortune, Phys. Rev. C **94**, 024339 (2016).

[25] S. S. Wang, Y. G. Ma, X. G. Cao, D. Q. Fang, and C. W. Ma, Phys. Rev. C **102**, 024620 (2020).

[26] Y. Z. Sun, S. T. Wang, Y. P. Xu, D. Y. Pang, G. Li, C. X. Yuan, L. F. Wan, Y. Qiao, Y. Q. Wang, and X. Y. Chen, Phys. Rev. C **106**, 034614 (2022).

[27] E. K. Warburton and B. A. Brown, Phys. Rev. C **46**, 923 (1992).

[28] N. Shimizu, T. Mizusaki, Y. Utsuno, and Y. Tsunoda, Comput. Phys. Commun. **244**, 372 (2019).

[29] J. M. Boillos, D. Cortina-Gil, J. Benlliure, J. L. Rodríguez-Sánchez, H. Alvarez-Pol, L. Atar, T. Aumann *et al.*, Phys. Rev. C **105**, 014611 (2022).

[30] L. Atar, S. Paschalis, C. Barbieri, C. A. Bertulani, P. Díaz Fernández, M. Holl, M. A. Najafi, V. Panin *et al.*, Phys. Rev. Lett. **120**, 052501 (2018).

[31] M. Gómez-Ramos and A. Moro, Phys. Lett. B **785**, 511 (2018).

[32] Nguyen Tri Toan Phuc, K. Yoshida, and K. Ogata, Phys. Rev. C **100**, 064604 (2019).